

– For internal NASA and partners use only –

Total Ionizing Dose Estimate of the Solar Cruiser Reaction Control Device

Anthony M. DeStefano
NASA, MSFC, EV44

June 9, 2021

Contents

1 Executive Summary	1
2 Mission Trajectory	2
3 Materials	2
4 Dose-Depth in Kapton	2
4.1 Protons	2
4.2 Electrons	5
5 Natural Environments	6
5.1 Solar Particle Events	6
5.2 Low-Energy Solar Wind	8
6 Total Ionizing Dose	10
6.1 Solar Particle Events	11
6.1.1 Total Ionizing Dose vs. Material Depth	12
6.1.2 Total Ionizing Dose vs. Proton Energy	14
6.2 Low-Energy Solar Wind	16
6.2.1 Total Ionizing Dose vs. Material Depth	16
6.2.2 Total Ionizing Dose vs. Proton Energy	18
7 Results	20
References	21
A Dose Percentile-Depth vs. Energy Parameters Fits	22

B Raw L2-CPE output of the Interplanetary Proton Environment	23
--	----

List of Figures

1 Example of TRIM setup.	3
2 Left axis: Depth in Kapton vs. proton energy for various dose-depth percentiles. Right axis: Dose per proton fluence vs. energy.	4
3 The dose per fluence of protons is compared between SRIM (blue circles) and <i>Pelliccioni</i> [2000] (orange triangles).	5
4 Screen shot of the setup used in computing the low-energy proton flux environment in L2-CPE.	8
5 The differential TID vs. depth for a 11-month isotropic SPE environment at 0.984 AU in $150\mu\text{m}$ of Kapton.	12
6 The integral TID (less than a certain depth) vs. depth for a 11-month isotropic SPE environment at 0.984 AU in $150\mu\text{m}$ of Kapton.	13
7 The differential TID vs. energy for a 11-month isotropic SPE environment at 0.984 AU in $150\mu\text{m}$ of Kapton.	14
8 The integral TID (greater than a certain energy) vs. energy for a 11-month isotropic SPE environment at 0.984 AU in $150\mu\text{m}$ of Kapton.	15
9 The differential TID vs. depth for a 11-month isotropic background solar wind environment at 0.984 AU in $150\mu\text{m}$ of Kapton.	16
10 The integral TID (less than a certain depth) vs. depth for a 11-month isotropic background solar wind environment at 0.984 AU in $150\mu\text{m}$ of Kapton.	17
11 The differential TID vs. energy for a 11-month isotropic background solar wind environment at 0.984 AU in $150\mu\text{m}$ of Kapton.	18
12 The integral TID (greater than a certain energy) vs. energy for a 11-month isotropic background solar wind environment at 0.984 AU in $150\mu\text{m}$ of Kapton	19

List of Tables

1 Composition of Kapton.	2
2 Angular weight factors w_i where $\sum_i w_i = 1$. The θ_i and θ_{i+1} are bin edges where θ is taken as the approximate bin center.	10
3 Parameter fits to Equation (1) for various dose percentiles using normally incident protons.	22

Listings

1 ESP-PSYCHIC total fluence of protons for 11 months during solar maximum at 0.984 AU. The energy center = $\sqrt{\text{bin left edge} \times \text{bin right edge}}$.	7
---	---

2	The 95% sunward solar wind environment from L2-CPE for 11 months. The energy center = $\sqrt{\text{bin left edge} \times \text{bin right edge}}$	8
3	The sunward facing flux (worst-case) during solar maximum from IMP8 using L2-CPE.	23

1 Executive Summary

The total ionizing dose (TID) in the reaction control device (RCD) material of Solar Cruiser is estimated. A nominal mission length of 11 months is assumed at the sub-Sun-Earth L1 point (~ 0.984 AU). The RCD is assumed to be made of kapton with a thickness of $150\mu\text{m}$. Two components of the interplanetary natural environments were incorporated in this study, the solar particle events (SPEs) and the background solar wind. The TID from the high-energy ($>\text{GeV}$) cosmic rays was assumed to be negligible due to the thin materials studied in this analysis. It was found that proton energies beyond roughly 13.1 MeV would not deposit significant dose (i.e., less than 5% of the available dose) into the kapton material since the Bragg peak would be avoided. Taking into account an isotropic environment onto a flat slab (modeled as a cosine law), the TID from SPEs was 626 krads whereas the TID from the background solar wind was 11.0 krads, for a total of 637 krads. If an additional factor of $2\times$ is introduced, the estimated TID to $150\mu\text{m}$ of kapton is 1.27 Mrads.

2 Mission Trajectory

The nominal Solar Cruiser location is beyond the Sun-Earth L1 point, called sub-L1, roughly 0.984 AU from the Sun. The sub-L1 location is in interplanetary space with no shielding from any planetary bodies and is exposed to the solar wind. The nominal mission length is 11 months (assumed to be 335 days).

3 Materials

The representative material for the Reaction Control Device (RCD) of Solar Cruiser is $150\mu\text{m}$ of Kapton. Using data from NIST¹, the composition of Kapton is shown in Table 1, where the density of Kapton is 1.42 g/cm^3 .

Table 1: Composition of Kapton.

Atomic #	Fraction by Weight	Weight (amu)	Fraction by Number	Stoichiometry
1	0.026362	1.008	0.25639	10
6	0.691133	12.011	0.56412	22
7	0.073270	14.007	0.05128	2
8	0.209235	15.999	0.12821	5

4 Dose-Depth in Kapton

4.1 Protons

The SRIM (Stopping and Range of Ions in Solids) software is used to compute the dose in thin materials with no prior shielding. The SRIM software package contains TRIM (the Transport of Ions in Matter) [Ziegler, 2004; Ziegler *et al.*, 2010], with a screenshot of the setup used in this analysis shown in Figure 1.

The dose deposited in Kapton depends on the energy of the incident protons. As the energy increases, the depth of the deposited dose increases. In Figure 2, the colored solid curves show the percentiles of dose deposited less than a particular depth, as a function of energy for normally incident protons. For example, the purple curve shows the depth vs. energy at which 95% of the dose is deposited. From Figure 2, it is clear that the dose is not deposited uniformly. Thicknesses between the green and blue curves, 45% of the dose is deposited, as well as between the green and purple curves. Therefore, 90% of the dose is deposited between the blue and purple curves. In general, the depth vs. energy profile has a double-power-law shape (depth in angstrom Å and energy in electron volts eV)

$$D(E) = \left(\frac{E}{a}\right)^b + \left(\frac{E}{c}\right)^d, \quad (1)$$

¹<https://physics.nist.gov/cgi-bin/Star/compos.pl?matno=179>

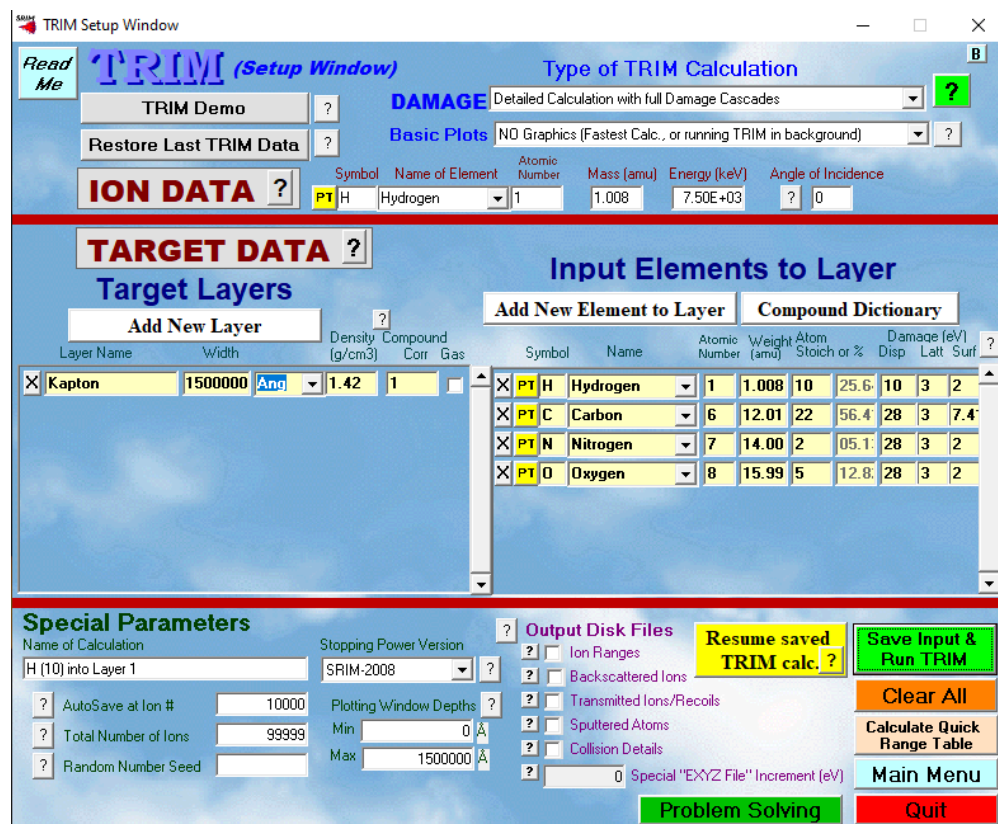


Figure 1: Example of TRIM setup.

where a is the low-energy scale, c is the high-energy scale, and b & d are the indices for each scale, respectively. As the percentile increases, the values for the energy scales a and c decreases. For a list of parameter fits, see Table 3 in Appendix A. Observing that $b < d$, the Kapton material is more effective at stopping lower energy protons ($<\sim 100$ keV) than higher energy protons.

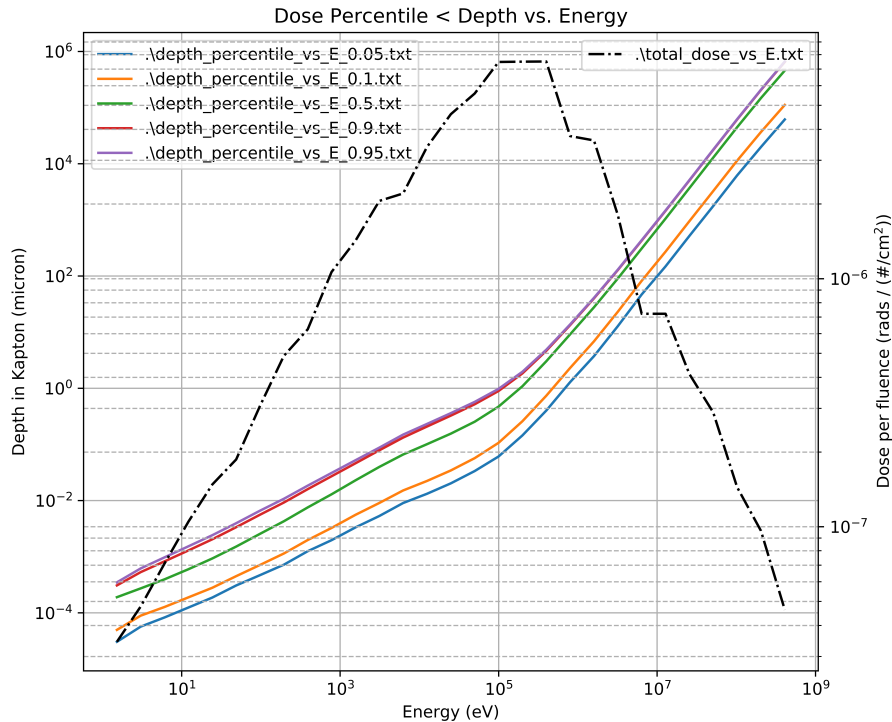


Figure 2: Left axis: Depth in Kapton vs. proton energy for various dose-depth percentiles. Right axis: Dose per proton fluence vs. energy.

The dotted-dashed curve in Figure 2 shows the total dose deposited per fluence as a function of energy. Basically, this curve can be thought of as the dose cross-section of Kapton for normally incident protons. One way to find the total dose for a given energy spectrum, one could convolute the dose cross-section with the differential energy spectrum, taking into account the depth percentile for a particular thickness of Kapton material. However, a more direct method to find the total dose is used in the following sections.

In Figure 3, Table A2.7 of [Pelliccioni \[2000\]](#) is compared with the dose per fluence curve from Figure 2 for incident protons. The ambient dose equivalent per unit fluence given in [Pelliccioni \[2000\]](#) is derived from the Monte Carlo code FLUKA [[Battistoni](#)

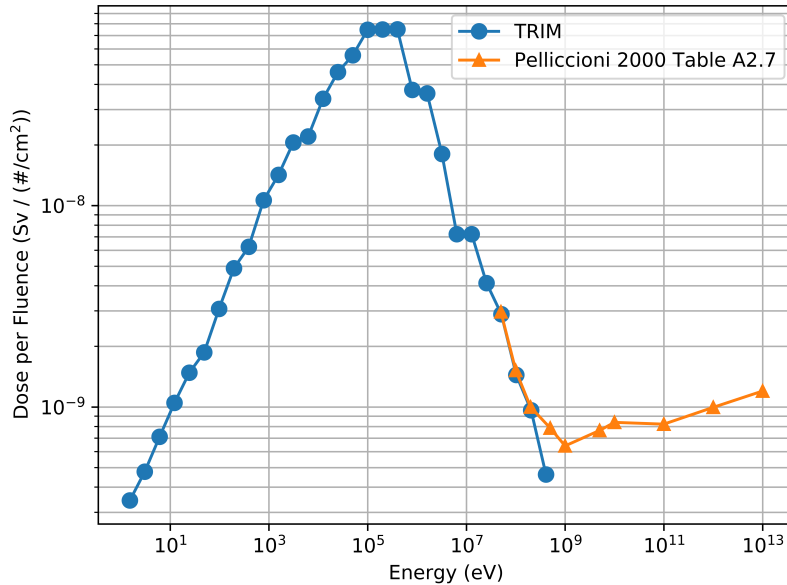


Figure 3: The dose per fluence of protons is compared between SRIM (blue circles) and *Pelliccioni* [2000] (orange triangles).

et al., 2015], termed *Pelliccioni conversion coefficients*². Both electronic and nuclear interactions are taken into account in the FLUKA code, in contrast with TRIM only handling electronic interactions. This difference in interactions explains why the dose per fluence curves deviate at the last blue marker at 0.41 GeV.

The agreement shown in Figure 3 also merits the factor of 0.01 required in converting the energy deposited to equivalent dose in Equation (4).

4.2 Electrons

²Used in the MULASSIS code, see <https://www.spenvis.oma.be/help/models/smul.html>.

5 Natural Environments

The natural environments for the RCD of Solar Cruiser are separated into a mid-energy component (solar energetic particles, Section 5.1) and a low-energy component (background solar wind, Section 5.2). The high-energy component (galactic cosmic rays, $>$ GeV) are omitted because of the thin materials studied in this analysis. In general, for an isotropic proton environment with energies greater than ~ 13.1 MeV (see Equation (6)), the particles do not deposit a significant amount of energy in $150\mu\text{m}$ Kapton (i.e., the Bragg peak has not been reached yet).

5.1 Solar Particle Events

The solar particle event (SPE) environment for interplanetary space is derived following the same procedure as outlined in the Cross-Program Design Specification for Natural Environments (DSNE) Section 3.3.1 (see the technical notes at the end of the section). A 11-month trajectory is defined in interplanetary space at the sub-L1 location of 0.984 AU in SPENVIS³ under the Coordinate generators tab. Once this is set, the SPE fluence is computed under the Solar particle mission fluences. The following parameters are set:

- Solar particle model: ESP-PSYCHIC (total fluence)
- Ion range: H to H
- Prediction period: automatic
- Offset in solar cycle: override
- Offset from solar maximum [years]: 0
- Confidence level [%]: 95.0

Note that the total fluence mode is used rather than the worst event fluence mode. In DSNE, the 1-year unshielded SPE (Table 3.3.1.10.2-1) uses the worst event fluence mode. However, in order to take into account the total dose due to all SPEs that occur in a particular time frame, the total fluence mode should be used. For example, the 15-year unshielded SPE TID environment (Table 3.3.1.10.2-5) uses the proton environment from ESP-PSYCHIC using the total fluence mode.

Listing 1 shows the down-selected energy bins that match DSNE Table 3.3.1.10.2-1. In terms of fluence > 100 keV, the 11-month SPE environment shown in Listing 1 is $2.3\times$ greater than the unshielded SPE environment in DSNE Table 3.3.1.10.2-1. This is why it is important to run the ESP-PSYCHIC model for the required mission length and not multiply Table 3.3.1.10.2-1 by the number of years. For the RCD material, the interest is in the total amount of accumulated dose, not the dose due to a worst-case event. For this reason, the 11-month environment derived here has a greater fluence than the 1-year SPE dose in DSNE.

³<https://www.spenvis.oma.be/>

Listing 1: ESP-PSYCHIC total fluence of protons for 11 months during solar maximum at 0.984 AU. The energy center = $\sqrt{\text{bin left edge} \times \text{bin right edge}}$.

#	Energy (keV)	Bin Flux (#/cm ²)	Energy width (keV)	Energy left edge (keV)
2	1.58E+02	5.21E+11	1.50E+02	1.00E+02
3	3.54E+02	2.25E+11	2.50E+02	2.50E+02
4	7.07E+02	1.40E+11	5.00E+02	5.00E+02
5	1.41E+03	8.71E+10	1.00E+03	1.00E+03
6	2.65E+03	4.85E+10	1.50E+03	2.00E+03
7	4.18E+03	2.55E+10	1.50E+03	3.50E+03
8	5.96E+03	2.06E+10	2.10E+03	5.00E+03
9	7.54E+03	6.06E+09	9.00E+02	7.10E+03
10	8.49E+03	5.24E+09	1.00E+03	8.00E+03
11	9.49E+03	4.14E+09	1.00E+03	9.00E+03
12	1.26E+04	1.49E+10	6.00E+03	1.00E+04
13	1.70E+04	2.77E+09	2.00E+03	1.60E+04
14	1.90E+04	2.12E+09	2.00E+03	1.80E+04
15	2.24E+04	3.81E+09	5.00E+03	2.00E+04
16	2.96E+04	4.07E+09	1.00E+04	2.50E+04
17	3.74E+04	1.15E+09	5.00E+03	3.50E+04
18	4.24E+04	8.49E+08	5.00E+03	4.00E+04
19	4.74E+04	6.36E+08	5.00E+03	4.50E+04
20	5.96E+04	1.48E+09	2.10E+04	5.00E+04
21	7.54E+04	3.26E+08	9.00E+03	7.10E+04
22	8.49E+04	2.57E+08	1.00E+04	8.00E+04
23	9.49E+04	1.84E+08	1.00E+04	9.00E+04
24	1.26E+05	4.48E+08	6.00E+04	1.00E+05
25	1.70E+05	5.64E+07	2.00E+04	1.60E+05
26	1.90E+05	3.88E+07	2.00E+04	1.80E+05
27	2.24E+05	5.64E+07	5.00E+04	2.00E+05
28	3.16E+05	5.23E+07	1.50E+05	2.50E+05
29	4.47E+05	9.04E+06	1.00E+05	4.00E+05

5.2 Low-Energy Solar Wind

To compute the low-energy solar wind plasma contribution of the environment, the L2-CPE V1.3 software package was used. By default, the environment is computed in interplanetary space around the Earth (i.e., at 1 AU), but a factor of $1/(0.984)^2 = 1.033$ is introduced to scale the fluences to the sub-L1 location. The proton fluence was computed with the setup shown in Figure 4. Other percentiles that are automatically calculated are 5%, 50%, 95%, and the maximum, mean, and minimum fluxes for each energy bin (see Listing 3 in Appendix B). Listing 2 shows the reduced data in the same format as Listing 1. The 95% is used in accordance with DSNE (see the technical notes at the end of Section 3.3.1). The sunward facing flux is used and assumed to be isotropic as worst-case.

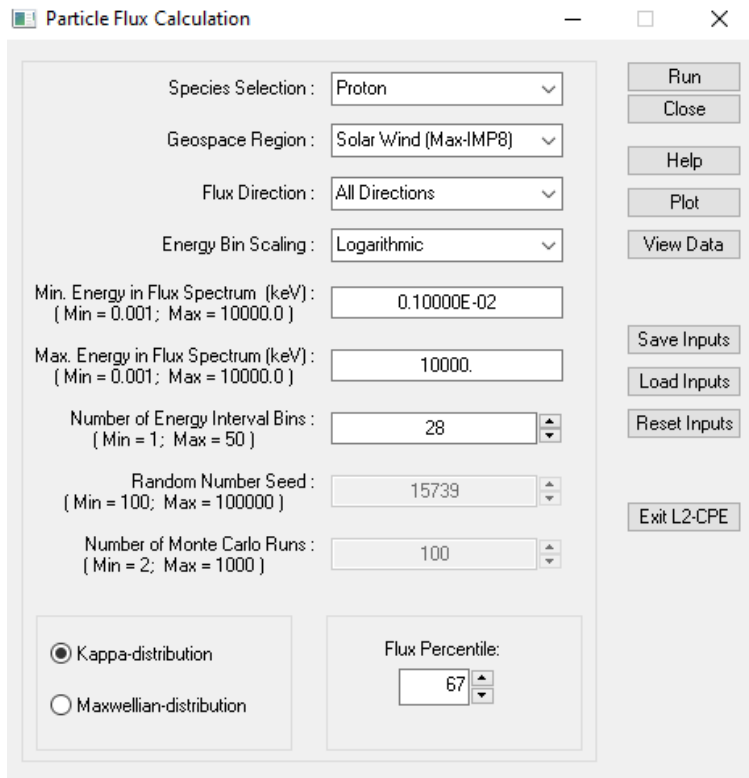


Figure 4: Screen shot of the setup used in computing the low-energy proton flux environment in L2-CPE.

Listing 2: The 95% sunward solar wind environment from L2-CPE for 11 months. The energy center = $\sqrt{\text{bin left edge} \times \text{bin right edge}}$.

#	Energy (keV)	Bin Flux (#/cm ²)	Energy width (keV)	Energy left edge (keV)
1	1.34E-03	2.35E+09	8.00E-04	1.00E-03
2	2.40E-03	3.96E+09	1.40E-03	1.80E-03

4	4.23E-03	6.54E+09	2.40E-03	3.20E-03
5	7.48E-03	1.06E+10	4.40E-03	5.60E-03
6	1.33E-02	1.66E+10	7.80E-03	1.00E-02
7	2.37E-02	2.51E+10	1.38E-02	1.78E-02
8	4.21E-02	3.63E+10	2.46E-02	3.16E-02
9	7.50E-02	4.97E+10	4.38E-02	5.62E-02
10	1.33E-01	6.48E+10	7.78E-02	1.00E-01
11	2.37E-01	7.78E+10	1.38E-01	1.78E-01
12	4.22E-01	8.81E+10	2.46E-01	3.16E-01
13	7.50E-01	9.17E+10	4.38E-01	5.62E-01
14	1.33E+00	8.89E+10	7.78E-01	1.00E+00
15	2.37E+00	7.97E+10	1.38E+00	1.78E+00
16	4.22E+00	6.63E+10	2.46E+00	3.16E+00
17	7.50E+00	5.20E+10	4.38E+00	5.62E+00
18	1.33E+01	3.89E+10	7.78E+00	1.00E+01
19	2.37E+01	2.72E+10	1.38E+01	1.78E+01
20	4.22E+01	1.85E+10	2.46E+01	3.16E+01
21	7.50E+01	1.21E+10	4.38E+01	5.62E+01
22	1.33E+02	7.81E+09	7.78E+01	1.00E+02
23	2.37E+02	4.92E+09	1.38E+02	1.78E+02
24	4.22E+02	3.04E+09	2.46E+02	3.16E+02
25	7.50E+02	1.85E+09	4.38E+02	5.62E+02
26	1.33E+03	1.11E+09	7.78E+02	1.00E+03
27	2.37E+03	6.75E+08	1.38E+03	1.78E+03
28	4.22E+03	4.02E+08	2.46E+03	3.16E+03
29	7.50E+03	2.39E+08	4.38E+03	5.62E+03

6 Total Ionizing Dose

The Stopping and Range of Ions in Matter (SRIM) is a group of programs that calculate the stopping and range of ions in matter⁴ [Ziegler, 2004; Ziegler et al., 2010]. For each run using TRIM (Transport of Ions in Matter), a mono-energetic beam of a single incident angle is used at the environment and transported through a series of predefined layers in a Monte Carlo fashion.

The isotropic flux for a particular energy and incident angle $\Phi(E, \theta)$ can be computed as (using a cosine distribution for an incident isotropic distribution on a flat slab)

$$\begin{aligned}\Phi(E, \theta) &= [\Phi(E_i) - \Phi(E_{i+1})] \frac{\cos(2\theta_i) - \cos(2\theta_{i+1})}{2}, \\ &= [\Phi(E_i) - \Phi(E_{i+1})] w_i,\end{aligned}\quad (2)$$

where $E = \sqrt{E_i E_{i+1}}$, $\theta = (\theta_i + \theta_{i+1})/2$, and $\Phi(E_i)$ is the integral flux at energy E_i (e.g., Section 5). The TRIM simulation is run using E and θ as centered values in the energy-angle bin. The angular weight term follows from the integral

$$w_i = 2 \int_{\theta_i}^{\theta_{i+1}} d\theta \sin \theta \cos \theta = \frac{\cos(2\theta_i) - \cos(2\theta_{i+1})}{2}, \quad (3)$$

where it is assumed that the incident angle θ ranges⁵ from 0° to 90° , hence the factor of 2. In this analysis, the range of incident angles θ are given in Table 2.

Table 2: Angular weight factors w_i where $\sum_i w_i = 1$. The θ_i and θ_{i+1} are bin edges where θ is taken as the approximate bin center.

index i	θ_i	θ_{i+1}	θ	w_i
0	0.00	15.0	0.00	3.40E-2
1	15.0	37.5	30.0	1.73E-1
2	37.5	52.5	45.0	1.85E-1
3	52.5	67.5	60.0	2.26E-1
4	67.5	82.5	75.0	2.52E-1
5	82.5	90.0	87.0	1.30E-1

TID can be computed by saving the ionization file once a sufficient number of test particles are run. The ionization file contains information about the deposited ionization energy due to the primary ions D_{ions} and to secondaries D_{recoils} (called recoils) as a function of target depth. The ionization energy units are in eV per Angstrom per ion. To convert the deposited energy into rads, as a function of incident ion energy, angle

⁴<http://www.srim.org/SRIM/SRIMINTRO.htm>

⁵Initially, the range of the incident angle is from -90° to 90° , but it is assumed the dose profiles will be symmetric about 0° .

and deposited depth, the following conversion equation is used

$$D(E, \theta, r) = [D_{\text{ions}} + D_{\text{recoils}}](E, \theta, r) \times \frac{10^8 \text{ \AA}}{\text{cm}} \times \frac{1.60218 \times 10^{-19} \text{ J}}{\text{eV}} \times \frac{Q_{\text{SRIM}} \Phi(E, \theta)}{\rho [\text{kg cm}^{-3}]} \times \frac{100 \text{ rads}}{\text{J/kg}}, \quad (4)$$

where $Q_{\text{SRIM}} = 0.01$ and ρ is the material density in units of kg cm^{-3} .

In Sections 6.1 and 6.2, the dose vs. depth and dose vs. energy curves are discussed for the solar particle events and low-energy solar wind, respectively. Note that the *rough* nature of the differential dose vs. depth curves found in Figures 5 and 9 are due to the finite number of incident energies and angles probed. Since the poorly resolved portion occurs at lower doses, the overall estimated TID should be numerically stable.

The integral dose vs. depth curves shown in Figures 6 and 10 can be interpreted as the dose deposited up to a particular depth (i.e., at that depth d or less than d towards the front facing surface).

In terms of energy, the integral dose vs. energy curves displayed in Figures 8 and 12 show the TID from particles incident with a particular energy E or greater. Since an isotropic flux environment is simulated, a clear break in the energy spectrum is not exactly seen. However, it is clear from the differential dose vs. energy plots (Figures 7 and 11) that the slope starts to fall off at around $E_{\text{crit}} = 4 \text{ MeV}$. This value of E_{crit} makes sense, because for $150 \mu\text{m}$ of Kapton at the 99 percentile of dose deposited, the corresponding energy is about 3.7 MeV. That is, using the fit parameters from Table 3 for the 99 percentile, omitting the low-energy terms (a and b), the energy can be solved as

$$E_{99\% \text{ dose}} = 1.393 \text{ keV} (D/1\text{\AA})^{0.554}, \quad (5)$$

where D is the thickness of the material (valid for $1 \mu\text{m} < D < 1 \text{ m}$) and E is the critical energy. For the upper limit of incident energy to deposit less than 5% of the total dose, the following equation can be used

$$E_{5\% \text{ dose}} = 4.543 \text{ keV} (D/1\text{\AA})^{0.560}, \quad (6)$$

giving $E_{5\% \text{ dose}} = 13.1 \text{ MeV}$ for $D = 150 \mu\text{m}$.

6.1 Solar Particle Events

The solar particle event (SPE) environment (from ESP-PSYCHIC) used in computing the total ionizing dose (TID) to $150 \mu\text{m}$ of Kapton can be found in Listing 1 (Section 5.1). Dose vs. depth is covered in Section 6.1.1 and Dose vs. energy in Section 6.1.2.

6.1.1 Total Ionizing Dose vs. Material Depth

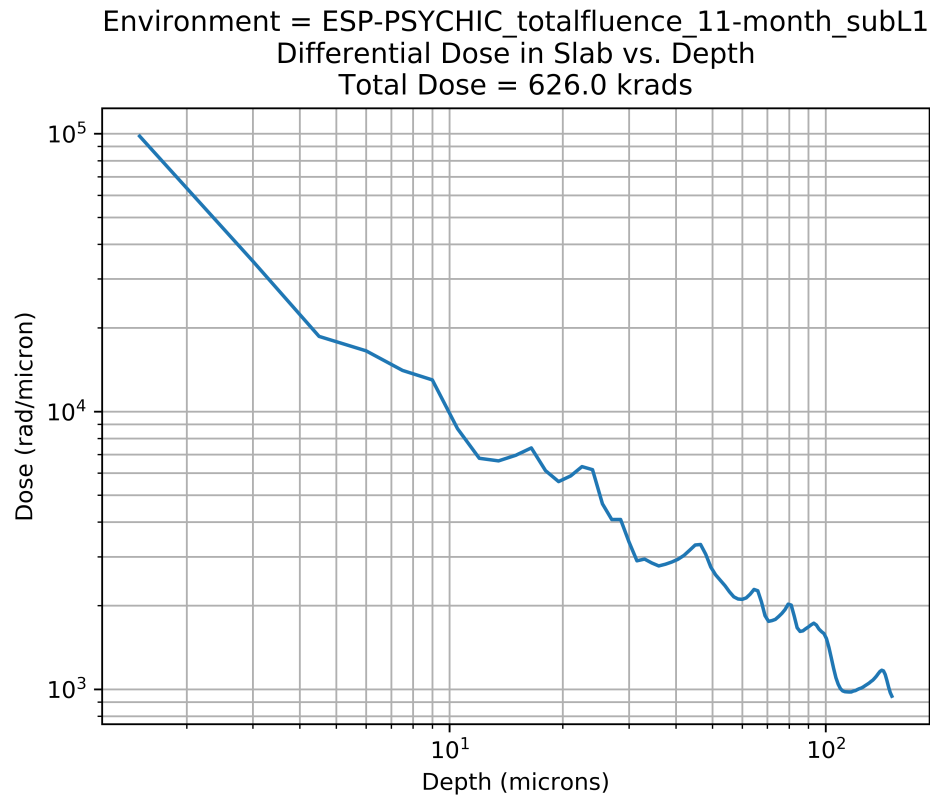


Figure 5: The differential TID vs. depth for a 11-month isotropic SPE environment at 0.984 AU in 150 μ m of Kapton.

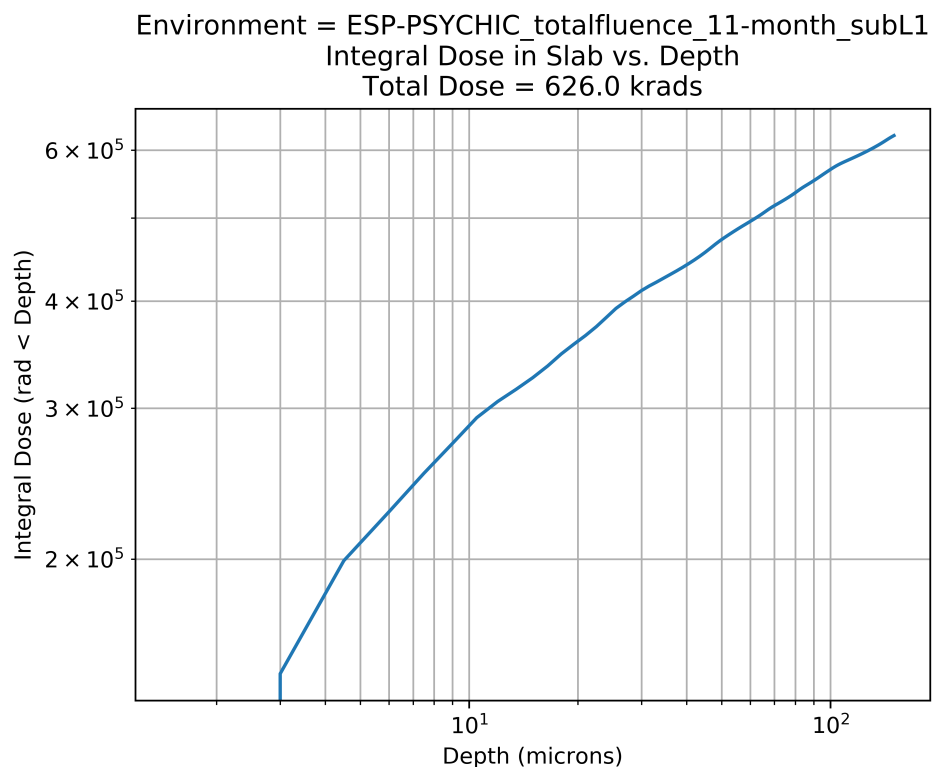


Figure 6: The integral TID (less than a certain depth) vs. depth for a 11-month isotropic SPE environment at 0.984 AU in 150 μ m of Kapton.

6.1.2 Total Ionizing Dose vs. Proton Energy

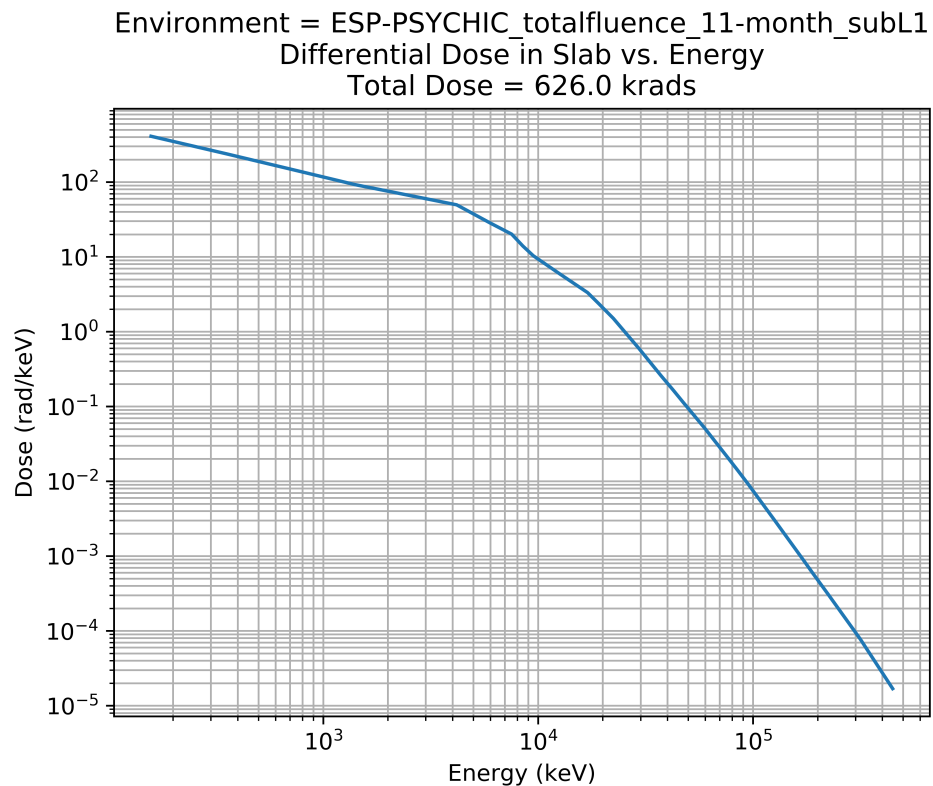


Figure 7: The differential TID vs. energy for a 11-month isotropic SPE environment at 0.984 AU in 150 μ m of Kapton.

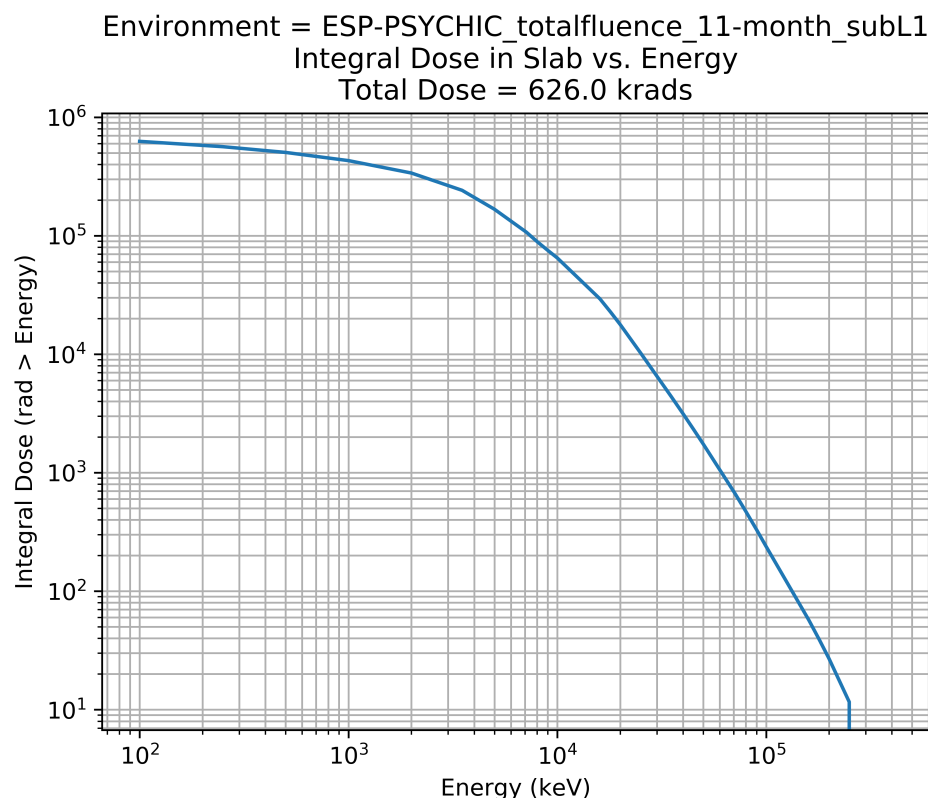


Figure 8: The integral TID (greater than a certain energy) vs. energy for a 11-month isotropic SPE environment at 0.984 AU in 150 μ m of Kapton.

6.2 Low-Energy Solar Wind

The low-energy solar wind environment (from L2-CPE) used in computing the TID to 150 μm of Kapton can be found in Listing 2 (Section 5.2). Dose vs. depth is covered in Section 6.2.1 and Dose vs. energy in Section 6.2.2.

6.2.1 Total Ionizing Dose vs. Material Depth

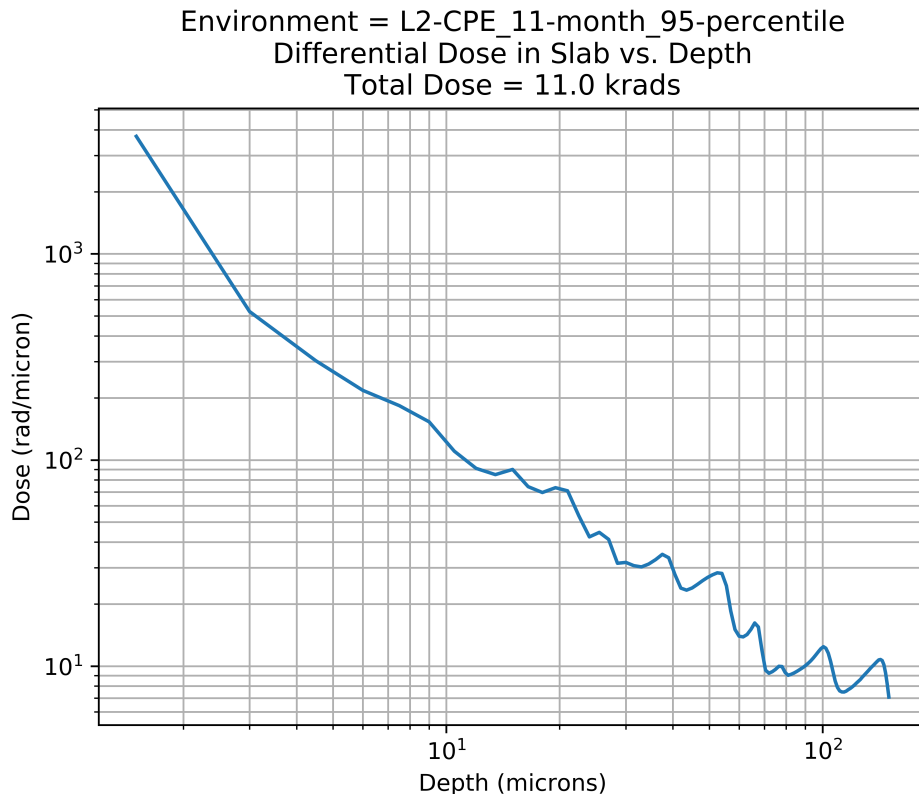


Figure 9: The differential TID vs. depth for a 11-month isotropic background solar wind environment at 0.984 AU in 150 μm of Kapton.

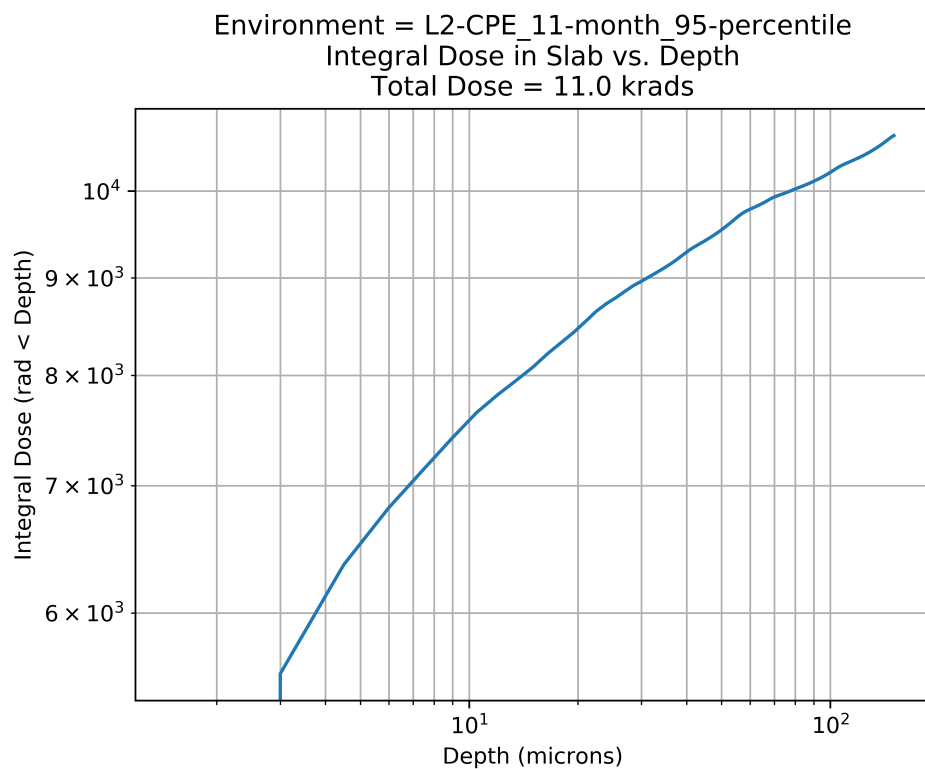


Figure 10: The integral TID (less than a certain depth) vs. depth for a 11-month isotropic background solar wind environment at 0.984 AU in 150 μ m of Kapton.

6.2.2 Total Ionizing Dose vs. Proton Energy

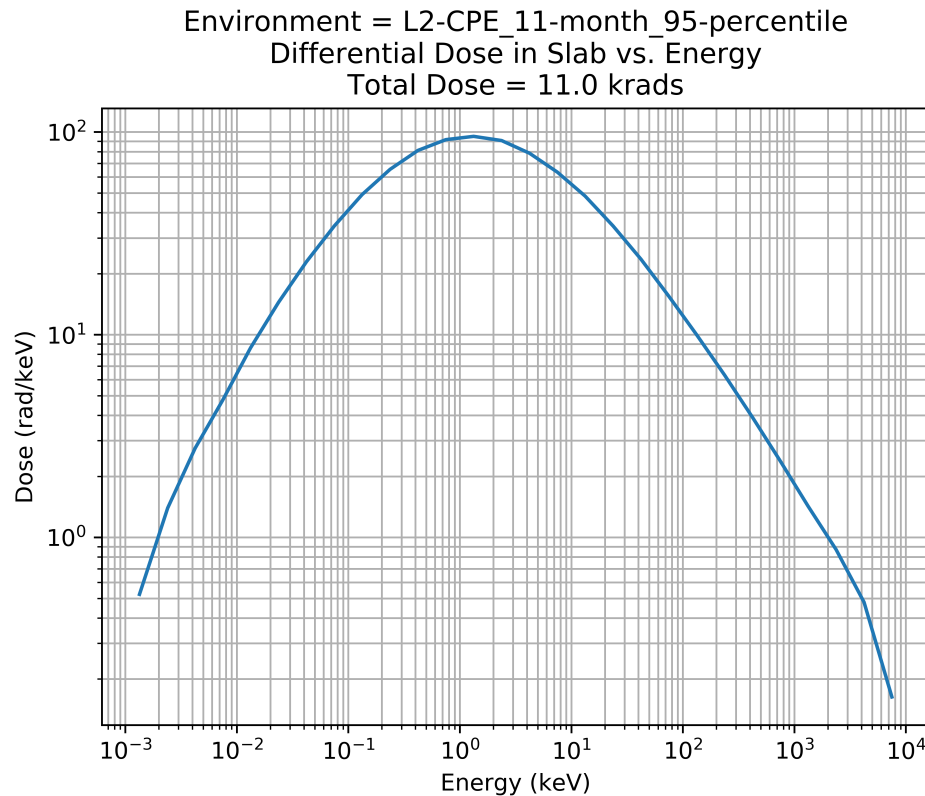


Figure 11: The differential TID vs. energy for a 11-month isotropic background solar wind environment at 0.984 AU in $150\mu\text{m}$ of Kapton.

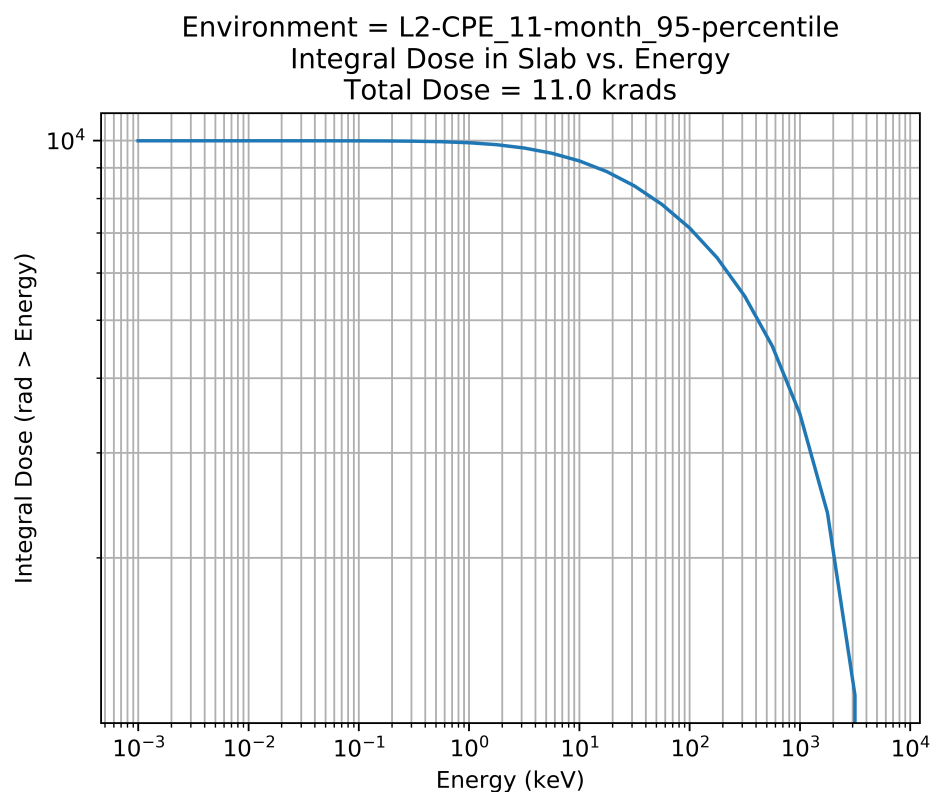


Figure 12: The integral TID (greater than a certain energy) vs. energy for a 11-month isotropic background solar wind environment at 0.984 AU in 150 μ m of Kapton

7 Results

The overall total ionizing dose (TID) in $150\mu\text{m}$ of Kapton (as defined in Section 3) from both the solar particle events (SPEs) (Section 5.1, TID of 626 krads) and the background solar wind (Section 5.2, TID of 11 krads) for 11 months in interplanetary space comes to **637 krads**. The driving factor is the SPE environment, which is assumed to be at solar maximum at a confidence level of 95%. The TID due to both heavy ions and electrons is omitted in this study.

Before the low-energy background solar wind was analyzed, it was unclear whether it would be a driver or not. Due to the thin layer of Kapton, it was expected only the mid- to low-energy component (i.e., < 13.1 MeV) would contribute to the TID. However, the results show that the background solar wind component provides only 1.7% of the overall TID.

According to Figure 6 for the SPE environment, roughly 20% of the overall TID occurs in the first $3\mu\text{m}$ of the kapton material, whereas for the background solar wind, Figure 10 shows that roughly 60% of the overall TID occurs in the first $3\mu\text{m}$. This is consistent with the fact that the SPE environment has more higher energy protons than the background solar wind environment, and therefore will penetrate further into the kapton material. Given that a majority of the dose is deposited in the outermost layer of kapton, any thin film over the RCD might protect the inner layers from TID, especially due to the background solar wind.

References

- Battistoni, G., et al., Overview of the fluka code, *Annals of Nuclear Energy*, 82, 10–18, 2015.
- Pelliccioni, M., Overview of fluence-to-effective dose and fluence-to-ambient dose equivalent conversion coefficients for high energy radiation calculated using the fluka code, *Radiation Protection Dosimetry*, 88(4), 279–297, 2000.
- Ziegler, J. F., Srim-2003, *Nuclear instruments and methods in physics research section B: Beam interactions with materials and atoms*, 219, 1027–1036, 2004.
- Ziegler, J. F., M. D. Ziegler, and J. P. Biersack, Srim—the stopping and range of ions in matter (2010), *Nuclear Instruments and Methods in Physics Research Section B: Beam Interactions with Materials and Atoms*, 268(11-12), 1818–1823, 2010.

A Dose Percentile-Depth vs. Energy Parameters Fits

Table 3: Parameter fits to Equation (1) for various dose percentiles using normally incident protons.

Percentile/100	<i>a</i>	<i>b</i>	<i>c</i>	<i>d</i>
0.05	8.445E+00	6.539E-01	4.543E+03	1.785E+00
0.10	4.414E+00	6.654E-01	3.267E+03	1.786E+00
0.15	2.923E+00	6.729E-01	2.682E+03	1.787E+00
0.20	2.171E+00	6.793E-01	2.339E+03	1.788E+00
0.25	1.723E+00	6.845E-01	2.109E+03	1.789E+00
0.30	1.429E+00	6.894E-01	1.947E+03	1.790E+00
0.35	1.216E+00	6.937E-01	1.826E+03	1.792E+00
0.40	1.057E+00	6.976E-01	1.732E+03	1.793E+00
0.45	9.332E-01	7.013E-01	1.658E+03	1.794E+00
0.50	8.296E-01	7.043E-01	1.598E+03	1.795E+00
0.55	7.407E-01	7.067E-01	1.549E+03	1.796E+00
0.60	6.660E-01	7.089E-01	1.510E+03	1.798E+00
0.65	6.006E-01	7.109E-01	1.479E+03	1.799E+00
0.70	5.423E-01	7.128E-01	1.456E+03	1.800E+00
0.75	4.868E-01	7.140E-01	1.438E+03	1.801E+00
0.80	4.309E-01	7.141E-01	1.423E+03	1.802E+00
0.85	3.744E-01	7.131E-01	1.412E+03	1.803E+00
0.90	3.140E-01	7.104E-01	1.402E+03	1.804E+00
0.95	2.441E-01	7.046E-01	1.396E+03	1.804E+00
0.99	1.554E-01	6.904E-01	1.393E+03	1.805E+00
0.999	9.998E-02	6.752E-01	1.394E+03	1.807E+00
0.9999	7.282E-02	6.638E-01	1.385E+03	1.806E+00

B Raw L2-CPE output of the Interplanetary Proton Environment

Listing 3: The sunward facing flux (worst-case) during solar maximum from IMP8 using L2-CPE.

```

1                                         - FLUX SUMMARY -
2   L2-CPE V1.3          Kappa-distribution
3   Cartesian (LRAD) Algorithm
4
5
6   Phenomenological Region => Solar Wind at SolMax (IMP-8)
7
8
9
10  Species => Protons
11
12  Positive X direction flux calculated.
13
14  Minimum Energy =      0.0010 keV
15  Maximum Energy = 10000.0000 keV
16
17  Number of Energy Bins =    28
18
19  50% Total Flux      =  0.6109E+03 (#/cm^2/sec)
20  95% Total Flux      =  0.2986E+05 (#/cm^2/sec)
21  5% Total Flux       =  0.6493E+01 (#/cm^2/sec)
22  67% Total Flux      =  0.1896E+04 (#/cm^2/sec)
23  Maximum Total Flux  =  0.5679E+07 (#/cm^2/sec)
24  Minimum Total Flux  =  0.1387E-02 (#/cm^2/sec)
25  Mean Total Flux     =  0.7319E+04 (#/cm^2/sec)
26  Std. Dev. Total Flux =  0.4616E+05 (#/cm^2/sec)
27
28
29                                         Differential Energy Flux Table (#/cm^2/sec/keV)
30
31
32
33
34
35
36
37
38
39
40

```

E1(keV)	E2(keV)	50%	95%	5%	67%
Maximum	Minimum	Mean	Std. Dev.		
0.0010	0.0018	0.4228E+04	0.1013E+06	0.8432E+02	0.1078E+05
+08	0.2333E-01	0.2406E+05	0.1700E+06		0.4149E
0.0018	0.0032	0.3944E+04	0.9578E+05	0.7729E+02	0.1009E+05
+08	0.2121E-01	0.2272E+05	0.1597E+06		0.3867E
0.0032	0.0056	0.3597E+04	0.8902E+05	0.6892E+02	0.9277E+04
+08	0.1871E-01	0.2109E+05	0.1472E+06		0.3526E
0.0056	0.0100	0.3200E+04	0.8097E+05	0.5914E+02	0.8297E+04
+08	0.1588E-01	0.1914E+05	0.1324E+06		0.3125E
0.0100	0.0178	0.2742E+04	0.7134E+05	0.4856E+02	0.7171E+04
+08	0.1282E-01	0.1688E+05	0.1155E+06		0.2671E
0.0178	0.0316	0.2252E+04	0.6065E+05	0.3763E+02	0.5959E+04
+08	0.9715E-02	0.1437E+05	0.9709E+05		0.2182E
0.0316	0.0562	0.1746E+04	0.4935E+05	0.2715E+02	0.4692E+04
+08	0.6801E-02	0.1173E+05	0.7806E+05		0.1685E
0.0562	0.1000	0.1268E+04	0.3808E+05	0.1798E+02	0.3485E+04
+08	0.4322E-02	0.9100E+04	0.5960E+05		0.1216E
0.1000	0.1778	0.8508E+03	0.2786E+05	0.1078E+02	0.2404E+04
+07	0.2350E-02	0.6656E+04	0.4296E+05		0.8108E

41	0.1778	0.3162	0.5214E+03	0.1882E+05	0.5686E+01	0.1526E+04	0.4940E
42	+07	0.1078E-02	0.4558E+04	0.2909E+05			
43	0.3162	0.5623	0.2876E+03	0.1200E+05	0.2641E+01	0.8831E+03	0.2727E
44	+07	0.4226E-03	0.2905E+04	0.1846E+05			
45	0.5623	1.0000	0.1428E+03	0.7016E+04	0.1063E+01	0.4634E+03	0.1357E
46	+07	0.1060E-03	0.1717E+04	0.1096E+05			
47	1.0000	1.7783	0.6332E+02	0.3824E+04	0.3668E+00	0.2177E+03	0.6088E
48	+06	0.2191E-04	0.9409E+03	0.6094E+04			
49	1.7783	3.1623	0.2496E+02	0.1928E+04	0.1092E+00	0.9264E+02	0.2900E
50	+06	0.3786E-05	0.4789E+03	0.3183E+04			
51	3.1623	5.6234	0.8762E+01	0.9028E+03	0.2810E-01	0.3574E+02	0.1467E
52	+06	0.5546E-06	0.2276E+03	0.1569E+04			
53	5.6234	10.0000	0.2794E+01	0.3977E+03	0.6305E-02	0.1251E+02	0.7069E
54	+05	0.7017E-07	0.1018E+03	0.7351E+03			
55	10.0000	17.7828	0.8167E+00	0.1673E+03	0.1265E-02	0.4048E+01	0.3331E
56	+05	0.7825E-08	0.4326E+02	0.3295E+03			
57	17.7828	31.6228	0.2200E+00	0.6582E+02	0.2297E-03	0.1225E+01	0.1518E
58	+05	0.7849E-09	0.1764E+02	0.1422E+03			
59	31.6228	56.2341	0.5576E-01	0.2516E+02	0.3830E-04	0.3482E+00	0.6881E
60	+04	0.7220E-10	0.6967E+01	0.5949E+02			
61	56.2341	100.0000	0.1341E-01	0.9267E+01	0.5868E-05	0.9401E-01	0.2985E
62	+04	0.6195E-11	0.2690E+01	0.2427E+02			
63	100.0000	177.8279	0.3090E-02	0.3361E+01	0.8546E-06	0.2441E-01	0.1249E
64	+04	0.5030E-12	0.1023E+01	0.9707E+01			
65	177.8279	316.2278	0.6874E-03	0.1191E+01	0.1201E-06	0.6135E-02	0.5097E
66	+03	0.3913E-13	0.3849E+00	0.3827E+01			
67	316.2278	562.3413	0.1495E-03	0.4141E+00	0.1598E-07	0.1510E-02	0.2056E
68	+03	0.2944E-14	0.1441E+00	0.1493E+01			
69	562.3413	1000.0000	0.3152E-04	0.1416E+00	0.2079E-08	0.3623E-03	0.8160E
70	+02	0.2159E-15	0.5386E-01	0.5782E+00			
71	1000.0000	1778.2794	0.6590E-05	0.4795E-01	0.2656E-09	0.8677E-04	0.3197E
72	+02	0.1552E-16	0.2013E-01	0.2229E+00			
73	1778.2794	3162.2776	0.1354E-05	0.1634E-01	0.3325E-10	0.2047E-04	0.1240E
74	+02	0.1100E-17	0.7536E-02	0.8573E-01			
75	3162.2776	5623.4131	0.2765E-06	0.5473E-02	0.4064E-11	0.4813E-05	0.4777E
76	+01	0.6855E-19	0.2829E-02	0.3294E-01			
77	5623.4131	10000.0000	0.5583E-07	0.1828E-02	0.4980E-12	0.1122E-05	0.1829E
78	+01	0.3413E-20	0.1066E-02	0.1266E-01			
79							
80							
81							
82							
83							
84							
85							
86							
87							
88							
89							
90							
91							
92							
93							
94							
95							
96							
97							
98							
99							
100							
101							
102							
103							
104							
105							
106							
107							
108							
109							
110							
111							
112							
113							
114							
115							
116							
117							
118							
119							
120							
121							
122							
123							
124							
125							
126							
127							
128							
129							
130							
131							
132							
133							
134							
135							
136							
137							
138							
139							
140							
141							
142							
143							
144							
145							
146							
147							
148							
149							
150							
151							
152							
153							
154							
155							
156							
157							
158							
159							
160							
161							
162							
163							
164							
165							
166							
167							
168							
169							
170							
171							
172							
173							
174							
175							
176							
177							
178							
179							
180							
181							
182							
183							
184							
185							
186							
187							
188							
189							
190							
191							
192							
193							
194							
195							
196							
197							
198							
199							
200							
201							
202							
203							
204							
205							
206							
207							
208							
209							
210							
211							
212							
213							
214							
215							
216							
217							
218							
219							
220							
221							
222							
223							
224							
225							
226							
227							
228							
229							
230							
231							
232							
233							
234							
235							
236							
237							
238							
239							
240							
241							
242							
243							
244							
245							
246							
247							
248							
249							
250							
251							
252							
253							
254							
255							
256							
257							
258							
259							
260							
261							
262							
263							
264							
265							
266				</td			

71	0.0316	0.0562	0.4296E+02	0.1215E+04	0.6682E+00	0.1155E+03	0.4147E
72	+06	0.1674E-03	0.2887E+03	0.1921E+04			
	0.0562	0.1000	0.5549E+02	0.1666E+04	0.7870E+00	0.1525E+03	0.5322E
73	+06	0.1891E-03	0.3983E+03	0.2608E+04			
	0.1000	0.1778	0.6622E+02	0.2169E+04	0.8392E+00	0.1871E+03	0.6310E
74	+06	0.1829E-03	0.5180E+03	0.3343E+04			
	0.1778	0.3162	0.7216E+02	0.2605E+04	0.7869E+00	0.2113E+03	0.6837E
75	+06	0.1492E-03	0.6308E+03	0.4026E+04			
	0.3162	0.5623	0.7079E+02	0.2952E+04	0.6500E+00	0.2173E+03	0.6712E
76	+06	0.1040E-03	0.7149E+03	0.4543E+04			
	0.5623	1.0000	0.6250E+02	0.3071E+04	0.4650E+00	0.2028E+03	0.5941E
77	+06	0.4638E-04	0.7516E+03	0.4797E+04			
	1.0000	1.7783	0.4928E+02	0.2976E+04	0.2854E+00	0.1694E+03	0.4738E
78	+06	0.1705E-04	0.7323E+03	0.4743E+04			
	1.7783	3.1623	0.3454E+02	0.2669E+04	0.1511E+00	0.1282E+03	0.4014E
79	+06	0.5240E-05	0.6628E+03	0.4405E+04			
	3.1623	5.6234	0.2156E+02	0.2222E+04	0.6916E-01	0.8797E+02	0.3611E
80	+06	0.1365E-05	0.5602E+03	0.3862E+04			
	5.6234	10.0000	0.1223E+02	0.1741E+04	0.2760E-01	0.5475E+02	0.3094E
81	+06	0.3071E-06	0.4456E+03	0.3217E+04			
	10.0000	17.7828	0.6356E+01	0.1302E+04	0.9842E-02	0.3150E+02	0.2593E
82	+06	0.6090E-07	0.3367E+03	0.2564E+04			
	17.7828	31.6228	0.3045E+01	0.9110E+03	0.3178E-02	0.1696E+02	0.2101E
83	+06	0.1086E-07	0.2441E+03	0.1968E+04			
	31.6228	56.2341	0.1372E+01	0.6192E+03	0.9425E-03	0.8571E+01	0.1693E
84	+06	0.1777E-08	0.1715E+03	0.1464E+04			
	56.2341	100.0000	0.5868E+00	0.4056E+03	0.2568E-03	0.4114E+01	0.1306E
85	+06	0.2711E-09	0.1177E+03	0.1062E+04			
	100.0000	177.8279	0.2405E+00	0.2616E+03	0.6651E-04	0.1900E+01	0.9719E
86	+05	0.3915E-10	0.7958E+02	0.7555E+03			
	177.8279	316.2278	0.9513E-01	0.1649E+03	0.1662E-04	0.8491E+00	0.7055E
87	+05	0.5415E-11	0.5327E+02	0.5296E+03			
	316.2278	562.3413	0.3678E-01	0.1019E+03	0.3933E-05	0.3717E+00	0.5061E
88	+05	0.7245E-12	0.3547E+02	0.3674E+03			
	562.3413	1000.0000	0.1380E-01	0.6197E+02	0.9101E-06	0.1586E+00	0.3571E
89	+05	0.9447E-13	0.2357E+02	0.2531E+03			
	1000.0000	1778.2794	0.5129E-02	0.3732E+02	0.2067E-06	0.6753E-01	0.2488E
90	+05	0.1208E-13	0.1567E+02	0.1735E+03			
	1778.2794	3162.2776	0.1874E-02	0.2261E+02	0.4601E-07	0.2833E-01	0.1717E
91	+05	0.1522E-14	0.1043E+02	0.1186E+03			
	3162.2776	5623.4131	0.6804E-03	0.1347E+02	0.1000E-07	0.1185E-01	0.1176E
92	+05	0.1687E-15	0.6963E+01	0.8106E+02			
	5623.4131	10000.0000	0.2443E-03	0.8000E+01	0.2180E-08	0.4910E-02	0.8007E
93	+04	0.1494E-16	0.4665E+01	0.5541E+02			
94	TOTALS:		0.5836E+03	0.2937E+05	0.6244E+01	0.1811E+04	0.6977E
	+07	0.1260E-02	0.7319E+04	0.5040E+05			